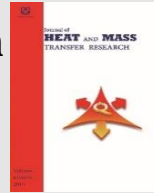




Semnan University



Research Article

A Two-Dimensional Cell Model of Phases Transport in a Fluidized Bed Column: Development and Validation

Andrey Mitrofanov

Independent researcher, Partizanski put b.b. 111a, 85355, Sutomore, Montenegro

ARTICLE INFO

Article history:

Received: 2024-07-13

Revised: 2024-12-11

Accepted: 2024-12-14

Keywords:

Fluidized bed;

Numerical simulation;

Markov chains;

Particulate solid;

Gas-solid transport.

ABSTRACT

Fluidized bed apparatuses are widely used in chemical engineering. Description of the hydrodynamic state of the apparatus is the starting point for predicting most technological operations in gas-solid flows. The object of this study is the gas and solids distributions in a fluidized bed column. The key aim of the study is to develop a simple yet informative mathematical model of the migration of gas and particulate solids in a fluidized bed column. The model is developed to solve the problem in a two-dimensional formulation. The phase migrations of the fluidized bed along the height of the column are described on the basis of the mathematical apparatus of the theory of Markov chains, and an explicit difference scheme is used for the mathematical model of particle transfer in the radial direction. A cell of small but finite size acts as a representative volume of the simulated system. The representative volume of such geometry is apparently used for modeling the motion of fluidized bed phases for the first time. At the same time, it is precisely this model structure that corresponds to the tradition of identifying the radial and axial coefficients of particle macrodiffusion. Parametric identification of the model is carried out on the basis of the empirical relationships known from the literature. The numerical experiments performed in the study showed the qualitative consistency of the proposed model. A comparison of calculations with the results of a natural experiment also confirmed the presence of predictive capabilities in the model. Thus, the proposed model can be considered as a reliable scientific basis for computer methods for calculating fluidized bed devices.

© 2025 The Author(s). Journal of Heat and Mass Transfer Research published by Semnan University Press.

This is an open access article under the CC-BY-NC 4.0 license. (<https://creativecommons.org/licenses/by-nc/4.0/>)

1. Introduction

Fluidized beds are widely used in the chemical and other fields of process engineering for a large variety of processes [1–5]. However the gas-solid contacting pattern in a fluidized bed is extremely complex, which leads to problems with design and operation fluidized bed devices [1,3,6].

In the literature, the different aspects of the gas-solid fluidization process have been extensively studied using different theoretical and experimental instruments [1,5,7,8]. The

bank of accumulated knowledge about the operation of fluidized bed units is practically inexhaustible [3,7,8] and has long acquired the properties of a «Shakespeare paradox» (that is, their volume is so large that it cannot be mastered by the human mind), which was already mentioned decades ago in the generalizing well-known book by Harrison and Davidson [3]. Certainly, since the publication of the mentioned generalizing book [3], the volume of this knowledge has increased significantly, and the current progress and understanding in the hydrodynamics and transport phenomena of

* Corresponding author.

E-mail address: mitrofanov3786@gmail.com

Cite this article as:

Mitrofanov, A. 2025. A Two-dimensional Cell Model of Phases Transport in a Fluidized Bed Column: Development and Validation. *Journal of Heat and Mass Transfer Research*, 12(2), pp. 193-208.

<https://doi.org/10.22075/JHMTR.2024.34734.1577>

fluidized beds are based on more widespread investigations but far from being exhausted.

It should be noted that the «fluidized bed» concept includes various forms of the state of the ensemble of particles, which are obtained as a result of the contact interaction of the suspended agent and particulate solid [3,10–12]. Classifications of bulk media have been developed that allow to speak with some confidence about how the gas-solid suspension will behave in the apparatus (the most well-known example is the Geldart classification [13], which, however, can also be subjected to reasonable criticism [14,15]). However, in all cases, practical technical systems consist of a number of hierarchically connected subsystems, with the hydrodynamic subsystem playing a decisive role in heat and mass transfer processes. Thus, a description of the hydrodynamic parameters of fluidization is necessary for a better understanding of the production process as a whole [1,3,4,8].

The entire spectrum of studies in the field of fluidization area can be qualitatively divided into experimental and theoretical.

Experimental invasive and noninvasive techniques can be employed to study the gas-solid flows in a fluidized bed [10,16–18], but noninvasive observation methods are more reliable and informative [16]. These noninvasive methods (first of all, such as magnetic resonance imaging, positron emission particle tracking etc.) provide valuable insight into fluidized beds due to the great level of its detalization and significantly deepen the understanding of the fluidization phenomenon [16,18].

The development and applicability of various computational tools for fluidization modeling have also been discussed in numerous papers [1,2,5,8,19–26]. However, progress in this field of theoretical research is less clear. One of the reasons is that when developing a mathematical model, increasing the degree of decomposition of a gas-solid flow doesn't always lead to an increase in the accuracy of the forecast and the adequacy of the description of the ensemble of particles [5,22,24,26–28].

Gas-solid fluidization systems are typically nonlinear, heterogeneous ones. Mobile clusters of particles of various configurations and scales form a certain distribution of particles in the volume of the fluidized bed [29]. This nature of the formation of the structure of a fluidized medium leads to the idea that the tool used to construct a mathematical model should allow a flexible approach to the spatial discretization of the modeling object [5,29].

Nowadays the most popular approach (and continuing to gain popularity [1]) for modeling of fluidization are built on the basis of

combination of a computational fluid dynamics (CFD) and a discrete element method (DEM). The original idea behind this approach is to introduce into circulation a conditionally infinitely small volume, so such simulations have a very high computational cost [7,9,19,21].

The requirement to develop approaches for constructing mathematical descriptions on a compromise scale of the processes modeling with granular matter is regularly discussed in research [26,30]. However, at the subject level, such works are rare, although the published results of simulations are quite encouraging [22,23,31]. In particular, there are practically no two-dimensional mathematical models of a fluidized bed based on a cellular representation of a fluidized bed. Although in the single work, where the efficiency of the DEM-CFD model and the stochastic Markov model are compared, it was shown that with comparable accuracy, the calculation speed of the stochastic model was 70 times faster than CFD-DEM [31]. However, these stochastic two-dimensional models apparently have not received further development, which is a significant gap in the development of approaches to fluidization modeling.

The authors point to the relatively low adaptability of the stochastic model to changing operating conditions as a limiting factor, while CFD-DEM shows relatively strong adaptability [31]. At the same time, it can be assumed that the indicated difficulties were a consequence of the choice of a flat two-dimensional fluidized bed, for which the bank of parameters is still limited, although devices of a similar configuration are used for laboratory installations [32,33].

In the context of this study, the author focuses on the description of the conventional bubble-free fluidized bed and the bubbling fluidized bed [11]. Due to this paper, the author hopes to contribute to filling the gaps in the development of fluidization models based on the use of a compromise modeling scale.

The main goals of the study are:

- 1) To develop a two-dimensional cellular model of a batch fluidized bed column to describe the movement of bed components in radial and axial directions;
- 2) To show that the adaptability of the proposed model is sufficiently high by identifying its parameters using data known from the literature;
- 3) To perform a preliminary verification of the developed model by comparing the obtained simulations with the data of a lab-scale experiment.

The compromise size of the calculation domain is ensured by using the mathematical apparatus of the theory of Markov chains. The ideology of Markov chains allows choosing the cell size based on the needs and tasks of modeling. Thus the final goal of the study is to develop a simple yet informative mathematical model of the migration of gas and particulate solid in axial and radial directions a fluidized bed column.

2. Theoretical Background

2.1. Concepts of Fluidized Bed Simulations

The theoretical approaches to the mathematical modeling of fluidization are very diverse. If we consider particles and a fluidizing agent as interpenetrating continuous media, it is logical to use the equations of hydromechanics with their initial and boundary conditions to describe them. This approach is ultimately realized in using of CFD [20,34–36]. Recently, CFD modeling has been used intensively for the creation of models of particulate transport in different units with fluidized beds. The Eulerian approach, or the so-called two-fluid model forms the theoretical concept of the CFD models. According to it, the solid flows are statistically averaged and treated as interpenetrating continua [34,37].

Conceptually opposite is the approach in which particles are considered as separate discrete elements. Within this approach, it is necessary to use the conservation laws for angular momentum and quantity of motion for an individual particle. This is the so-called discrete element method (DEM) [38–41]. Since the movement of particles in a fluidized bed occurs due to their contact interaction with the gas (liquid) flow, the gas flow must also be somehow described mathematically. For this reason, DEM models usually work in conjunction with CFD models (this combination is also called, in this case, the discrete particle method – DPM) [42–45].

Qualitatively, the combination of the two above-mentioned approaches (Lagrange-Euler) looks like an impeccable choice for constructing fluidization models. The application of this approach is very productive in terms of setting and researching scientific problems since various scenarios can be considered and plausible solutions can be obtained for analysis. However, this method cannot be considered productive for engineering problems. A real particle system consists of a large number of elements, which makes the calculations cumbersome [1,9].

It seems quite probable that the computational difficulties of the DEM-CFD models can be overcome with the development of computer technology. It also seems that the problems associated with the parametric identification of numerous parameters will be far from being resolved for a long time. Firstly, because there are just a lot of these parameters, their exact list depends both on the process being modeled and on the vision of the problem by a particular researcher (which parameters will be considered the characteristics of the first order of significance). Second, it is important that all parameters involved in the model be reliably quantified simultaneously. Thirdly, the procedures for identifying many parameters in such models are a scientific problem when the solution cannot be expressed by a short formula but often represents a certain concept within which particular solutions can be formed. The following are examples of such problems: definition of the contact point of particles and number of contacting elements, calculation of forces acting on particles, contact models and, etc. A comprehensive review of the advantages and disadvantages of CFD-DEM coupling methods can be found in scientific literature, and almost all authors point out that there are still some problems to be solved in the future [2,46].

Thus, the search for simplified numerical methods to describe the structure of a fluidized bed is still relevant. This largely determines the objectives of this study. It is necessary to propose a model of the fluidized bed structure, which, on the one hand, would make it possible to describe it as an object with distributed spatial characteristics but, on the other hand, would be much simpler in terms of the number of identification parameters and the difficulty of their determination.

Stochastic modeling methods for describing the movement of granular media are relatively often used in chemical engineering [25,47,48]. The most conceptually close to the model proposed here are the stochastic models proposed by Dehling et al. [24], Mitrofanov et al. [49], and Zhuang et al. [31]. However, in the works of Dehling et al. [24] and Mitrofanov et al. [49], one-dimensional models of a fluidized bed were proposed; accordingly, calculations allow one to judge only the distribution of phases of the bed along its height.

In the paper of Zhuang et al. [31] the task of fluidization modeling is solved in a two-dimensional formulation, and very complex forms of existence of a fluidized bed (with the formation and bubbles dynamics) are considered and the comparison is made with the results of DEM modeling.

From a methodological point of view, this work is very interesting, but a flat two-dimensional bed is considered, when the computational domain is a rectangular cell. This assumption seems quite justified, since the installations with flat bed are often used to study concentration fields in fluidized beds [33,50].

However cylindrical devices are more common in engineering practice. This geometry of the devices requires the construction of simple but informative two-dimensional mathematical models in terms of axial and radial (lateral) coordinates. It's in these terms that the intensity of mixing in a fluidized bed is usually discussed [51,52].

2.2. Solids Mixing in Fluidized Bed

The nature of the mixing of particles in a fluidized bed isn't completely understood [53,54]. However, some qualitative characteristics have been established quite definitely. Many researchers reported that the intensity of axial mixing is usually higher than lateral mixing [52,54,55]. For example, in the experiments [54], the axial solids mixing was two orders of magnitude faster than the lateral solids mixing. This follows quite logically from the recognition that gas bubbles are the basic mixing factor [54,56]. Despite the complexity of the mixing mechanism, when describing lateral mixing numerically, it is usually fitted to a 1D Fickian-type diffusion equation [54]. It can be mentioned that the values of the dispersion coefficient in the literature are very scattered [54,57]. It is customary to consider the lateral effective diffusion coefficient D_{sr} to be well correlated with an excess gas velocity $(U_0 - U_{mf})$, where the U_0 is superficial air velocity, and the U_{mf} is the minimum fluidization velocity.

It was reported [54] that the correlation of Borodulya et al. [58] predicts the experimental values of the lateral dispersion coefficient D_{sr} quite well. The correlation of Borodulya et al. has the following form [58]:

$$D_{sr} = 0.013H_0(U_0 - U_{mf}) \left(\frac{D_c}{H_0} \right)^{0.5} Fr^{-0.15} \quad (1)$$

where D_c is the equivalent bed diameter, and Fr is the Froude number.

The axial diffusion coefficient D_{sa} can be calculated from the relationship proposed by Esin&Altun [12]:

$$D_{sa} = 0.051 \left(\frac{U_0}{U_{mf}} \right) \cdot (U_0 - U_{mf})^{1.471} \quad (2)$$

3. Mathematical Model

It is convenient to consider the process of constructing a two-dimensional mathematical model of fluidization of a granular medium in a cylindrical apparatus as a combination of two models. The first of them describes the axial movement of particles while the second model describes the movement of the granular medium in the radial direction.

3.1. Mathematical Model of the Particle Movement along the Height of the Apparatus

The concept of the mathematical model proposed in our previous work [23] is used here in order to describe the gas and solid phase migration over the fluidized bed height. This model was developed by means of the Markov chain approach. The basic principles of how to use the theory to model processes with particulate solids are clearly described by H. Dehling et al. [22] and by H. Berthiaux and V. Mizonov et al. [36]. According to this approach, the volume of the apparatus is separated into n perfectly mixed cells of the length $\Delta y = H/n$, where H is the height of the column. These cells form a chain of cells characterized by the system state vector S . The state vector S characterizes the distribution of the observed additive property along the chain of cells. The basic principle of representing the apparatus with a Markov chain is illustrated schematically in Fig. 1.

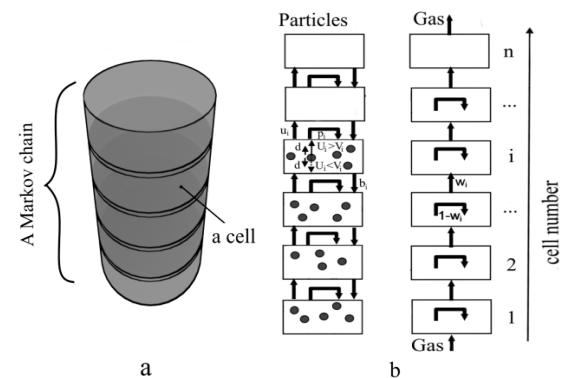


Fig. 1. General scheme for constructing the model of axial gas and solid transport in a fluidized bed: a) the general concept of representing the apparatus by a Markov chain; b) the diagram of possible movements of gas and solid phases of a fluidized bed

The system can include several observable additive properties, so several state vectors have to be introduced. Assume that the fluidized bed apparatus contains only uniform particles. Then, it will be enough to introduce into consideration the vectors only for gas and for particulate. So, for the one-dimension model (axial transport

model), the state vectors for particles (S) and for gas (S_g) are required. This scheme of the apparatus discretization is schematically shown in Fig. 1a and it corresponds to the one-dimensional cell model. Such models were considered in particular in [22,23].

The principle of such a model is not only to represent the vessel as several cells, which makes it possible to describe the distribution of the additive properties under consideration along the apparatus for a certain fixed moment in time. It is also important to study the transition between each of these cells over a certain time duration Δt . In other words, it is necessary to describe changes in the state vectors. With the discrete Markov chain model, we calculate the phase positions at discrete times only. The evolution of state vectors is described using recurrent matrix procedures. The next state vector is formed by multiplication of the transition matrix P (for solid phase) or P_g (for gas) on the current state vector (S and S_g correspond) until a steady state is reached [23].

To move from the one-dimensional fluidization model to the two-dimensional it is possible to repeat the above reasoning descriptions for N chains. In this case, each chain will describe the transfer of properties in the vertical direction not in the entire section of the apparatus, but only in one cylindrical layer.

The particle content distribution in the volume of apparatus is presented as the state massive $S=\{S_{r,i}\}$, where $r=1,2,\dots,N$ denotes the number of the cylindrical layer and $i=1,2,\dots,n$ denotes the number of the cell in the chain. For certain r the state vector $S_r=\{S_i\}$ determines the distribution of the material along the height of the r -th cylindrical layer. The common recurrent procedure for model particulate transport along the height of r -th cylindrical layer can be written in the following form [49,59]:

$$S_r^{k+1} = S_r^k \cdot P_r^k \tag{3}$$

where k is the time step number (the model calculates the evolution of the system state only for discrete moments of time $t_k = (k - 1) \cdot \Delta t$), and P_r is the transition matrix for particulate solid in the r -th layer [49].

A similar recurrent procedure for modeling gas transport along the height of r -th cylindrical layer is used [49,60]:

$$S_{g,r}^{k+1} = S_{g,r}^k \cdot P_{g,r}^k + F_r \tag{4}$$

where F is the source vector of the gas flow (contains one non-zero element equal to the amount of gas that during the time Δt is supplied to the first cell of the chain). If the vector F_r is the same for all r , then we have a uniform distribution of air velocities across the cross

section of the apparatus. In other words, the specific values of the elements of F for a given r determine the fluid velocity in the r -th cylindrical layer.

A rate of material exchange between the cells of the chains (along the height of r -th cylindrical layer) is described in probabilistic terms. It is necessary to know the values of these transition probabilities to a neighboring cell for each k -th moment of time. The possible transitions are staying in the same cell (p), moving upwards (u) to the next (located above) cell, and moving downward to the previous cell (b). These probabilities have to be related to the physical characteristics of particle transport. The proposed model uses the following assumptions. The procedure for calculating the local gas velocity during gas filtration through a section clogged with particles was proposed and verified within the framework of previous work [49]. The presence of particles in the apparatus's cross section (in each cell of the chain) naturally leads to the increase in the gas velocity. This, in turn, causes a decrease in the particulate concentration, which reduces the gas velocity. This continues until some equilibrium is established. The relationship between the particle content of particles and the gas velocity in a cell (indices are omitted) is given by the following ratio [49]:

$$U = \frac{U_0}{1 - \pi \left(\frac{S}{S_0 \cdot S_{max}} \right)^{2/3}} \tag{5}$$

where S and S_{max} are the corresponding k -th moment of time and the maximum (for a dense bed) values of the particle content in the cell (the indexes of the cell number and layer number are not given here, but calculation is made for each representative volume separately). The maximum content of particles with random packing S_{max} for a certain volume for a given particulate solid can be easily determined by simple tests with a bulk material [49,61].

The probabilities of a particle moving from the i -th cell forming the i -th column of the P transition matrix are related to the process parameters by the following dependencies [49]:

$$u_i = d_i \text{ for } U_i = V_i \tag{6}$$

$$u_i = d_i + (U_i - V_i)(\Delta t / \Delta y) \text{ for } U_i \geq V_i \tag{7}$$

$$b_i = d_i \text{ for } U_i > V_i \tag{8}$$

$$b_i = d_i + (V_i - U_i)(\Delta t / \Delta y) \text{ for } U_i \leq V_i, \tag{9}$$

$$p_i = 1 - b_i - u_i \tag{10}$$

where the aerodynamic size of the particle is characterized here by the particle settling velocity V , and the symmetrical part of transport probability d (diffusion probability) is calculated by the following relation [49,59]:

$$d_i = D_{sa} \cdot \Delta t / (\Delta y)^2 \quad (11)$$

The settling velocity V is related to the weight P of the particle as [49,60]:

$$P = 0.5 \cdot C_d \cdot f \cdot \rho_g \cdot V^2 \quad (12)$$

where C_d is the drag force coefficient, f is the area of the largest cross-section of a particle perpendicular to the velocity vector, ρ_g is the gas density. This parameter is not completely uniquely definable, and a comparative analysis of various models is possible for both a single particle and an ensemble of particles [62-64]. In this study, the reference point is taken on the following well-known dependence [64]:

$$C_d = (2.25 \cdot Re^{-0.31} + 0.36 \cdot Re^{0.06})^{0.45} \quad (13)$$

where Re is the dimensionless Reynolds number.

The above-mentioned probabilities for particulate transport allow forming of the matrix P (the indexes « r » for the layer number is not given here, but the calculations are made for each representative volume separately) in the following form [49,60]:

$$P = \begin{bmatrix} p_1 & b_2 & 0 & 0 & 0 \\ u_1 & p_2 & b_3 & 0 & 0 \\ 0 & u_2 & \dots & \dots & 0 \\ 0 & 0 & \dots & p_{n-1} & b_n \\ 0 & 0 & 0 & u_{n-1} & p_n \end{bmatrix} \quad (14)$$

The structure of the transition matrix is such that the fractions of particles remaining in the observed cell are located on the main diagonal of this matrix. The fractions of particles moving from the observed cell back (to the cell below) and upward (to the cell above) are placed on the diagonals located above and below the main one correspondently.

The transition matrix for gas is formed in a similar way. It is assumed that the gas flow moves in the plug-flow mode, so the transition matrix for each given cylindrical layer contains only two non-zero diagonals. The local gas velocity is calculated for each cell according to the relation (5) therefore the fraction of gas leaving the i -th cell during the time Δt can be represented in the following form [49,60]:

$$g_i = w_i \cdot \Delta t / \Delta y \quad (15)$$

Then, the matrix of transition probabilities for the gas phase will have the following form [49,59]:

$$P_g = \begin{bmatrix} 1-g_1 & 0 & 0 & 0 & 0 \\ g_1 & 1-g_2 & 0 & 0 & 0 \\ 0 & g_2 & \dots & 0 & 0 \\ 0 & 0 & \dots & 1-g_{n-1} & 0 \\ 0 & 0 & 0 & g_{n-1} & 1-g_n \end{bmatrix} \quad (16)$$

3.2. Mathematical Model of Lateral Particle Movement

The lateral particle migration is considered simplistically as a purely random walks (diffusion) process. From a formal mathematical point of view, such a problem is close to the description of radial thermal conductivity in a cylinder [65]. Fig. 2a shows a schematic diagram of the configuration of the computational domains. For each k -th time step, the state massive S_r is adjusted, taking into account the diffusion transport. When considering the balance of solids content in the r -th cell chain (cylindrical layer), it is taken into account that it borders neighboring layers with numbers $(r-1)$ and $(r+1)$. The volumes of bulk material transported in the radial direction are calculated as [61,65]:

For $r = 2, 3, \dots, N$:

$$q_{r-1,i}^k = \left[\frac{-D_{sr,i}^k}{\Delta r} \left(\frac{S_{r,i}^k}{V_{r,i}} - \frac{S_{r-1,i}^k}{V_{r-1,i}} \right) \right] (2\pi r_{r-1,i} \cdot \Delta y) \Delta t \quad (17)$$

For $r = 1, 2, \dots, N-1$:

$$q_{r+1,i}^k = \left[\frac{-D_{sr,i}^k}{\Delta r} \left(\frac{S_{r,i}^k}{V_{r,i}} - \frac{S_{r+1,i}^k}{V_{r+1,i}} \right) \right] (2\pi r_{r,i} \cdot \Delta y) \Delta t \quad (18)$$

The factors in square brackets on the left side of the equations (17)-(18) represent linear mass flux densities. Thus, the radial transport of particles is described in the usual way based on different formulations of the 1D Fickian-type model [65,66]. In this case, the terms in parentheses on the left side of equations (17)-(18) make it possible to take into account the radius-dependent transfer surface (domain shape) [49,61]:

$$\text{For } r = 2, 3, \dots, N-1 \quad S_r^{k+1} = S_r^k + q_{r-1}^k + q_{r+1}^k, \quad (19)$$

$$\text{For } r = 1 \quad S_r^{k+1} = S_r^k + q_{r+1}^k, \quad (20)$$

$$\text{For } r = N \quad S_r^{k+1} = S_r^k + q_{r-1}^k, \quad (21)$$

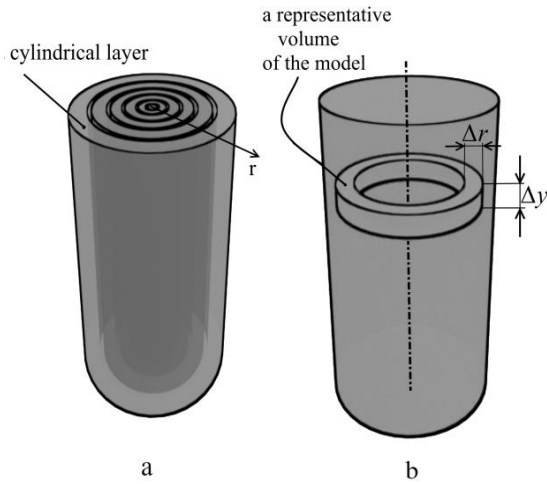


Fig. 2. General scheme for constructing the model: a) a schematic diagram of the configuration of the computational domains for a radial particulate transport; b) the computational domain for the proposed two-dimensional model

3.3. Mathematical Description of the 2-D Model of Particle Movement

The mathematical description of the two-dimensional fluidized bed model is based on a combination of the axial particle transport and the radial particle movement models. The final form of the computational domain for the proposed two-dimensional model is shown in Fig. 2b. The basic equation for this model of vertical migrations of particles is expression (3). And the resulting relations of the radial transport model are the equations (19)-(21). Their combination gives the following resulting equations [49,60,61]:

$$\text{For } r=2,3,\dots,N-1 \quad S_r^{k+1} = S_r^k \cdot P_r^k + q_{r-1}^k + q_{r+1}^k, \quad (22)$$

$$\text{For } r=1 \quad S_r^{k+1} = S_r^k \cdot P_r^k + q_{r+1}^k, \quad (23)$$

$$\text{For } r=N \quad S_r^{k+1} = S_r^k \cdot P_r^k + q_{r-1}^k, \quad (24)$$

4. Experimental Procedure

A drying column employed in another study was used for preliminary verification of the model. The kinetics of drying are not considered in this study. In fact an identical (triplicate realized) experiment on drying potato cubes with the side of 6 mm is considered. A continuous changes occurred in the fluidized bed structure due to particles dehydration (particles sizes and mass were changing). The experiments were carried out at the air temperature 70°C and the superficial gas velocity $U_0 = 5.5$ m/s.

A geometric sketch of the experimental setup is shown in Fig. 3.

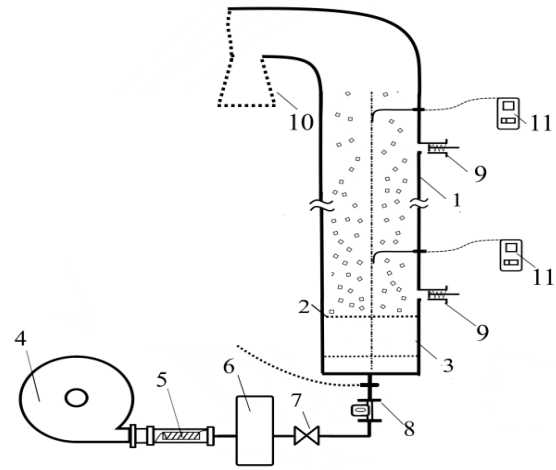


Fig. 3. General scheme for constructing the model: 1- fluidization column with internal diameter 0.1 m, 2 - gas distributor, 3 - plenum chamber, 4 - centrifugal blower, 5 - electrical heater, 6 - surge tank, 7 - control valve, 8 - flow meter, 9 - samplers, 10 - bag filter, 11 - Pitot tubes

The number of holes was made along the side of the column with a step of 0.1 m. Some of them were equipped with samplers to periodically collect samples of the material for weighing.

Three straight-type Pitot tubes were also used for measuring the local values of gas velocity in the fluidized bed. The measurements of the local gas velocity were taken at heights of 0.15 m, 0.35 m, and 0.55 m from the gas distribution plate. When measuring air velocities with a pitot tube, measurements were first taken on the axis of the apparatus, and then the tube was moved toward the wall of the column by 2.5 cm. The gas velocity values obtained in this way were recalculated using relation (5) in particle concentrations, which were compared with the model predictions.

The hydrodynamic local characteristics of the fluidized bed were measured for two points in time: after 10 minutes and after 55 minutes from the start of the drying process. The initial weight of the sample was 1.7 kg, with an average moisture content of 3.56 kg/kg. After 10 minutes of drying, the moisture content dropped to 2.5 kg/kg, and by 55 minutes of the drying process, it was about 0.12 kg/kg. As a result, the hydrodynamic situation in the bed changed dramatically. After 10 minutes of the process, the bed consisted of particles with an average size (5.6 mm) and a density of 1322 kg/m³. Such fluidized bed contained a small number of periodically appearing large gas bubbles, but in general, it was distinguished by the formation of large-scale particle flows within the bed, with a predominance of upward particle movement in the core of the bed and sliding down of particles at the periphery of the column. The minimum fluidization velocity U_{mf} of for the specified particles (to determine it, the process was

stopped and restarted with a gradual increase in gas rate to the operating velocity) was 2.4 m/s.

After 55 minutes of the process, the bed consisted of particles with an average size (4.2 mm) and a density of 646 kg/m³. The minimum fluidization velocity U_{mf} for the specified particles was 1.3 m/s. In this case, a few centimeters from the distributor, an obvious dense zone of the bed formed, in which the particles were actively mixed by gas bubbles. Apparently, due to the square shape, the particles actively rotated relative to their own axes, so their movement in the dense phase of the bed was very chaotic, and the gas bubbles collapsed extremely quickly. A zone of diluted fluidized bed without bubbles was formed above the dense phase. It was visually noticeable here that the concentration of particles decreased with height tending to zero.

The dimensionless operation velocity U_{mf}/U_0 for the specified modes were 2.3 and 4.2.

5. Results and Discussions

5.1. Numerical Experiments

The equalities (22)-(24) are the basic dependencies for the proposed model of balance equations. However, the type of solution largely depends on how to approach the issues of parametric identification when determining the model parameters.

The following scenario was considered in the numerical experiment. The cylindrical apparatus is filled with spherical particles with $d_p=2.5$ mm and a true material density of $\rho_p=1800$ kg/m³. The column of the apparatus is of 20 cm in height and 10.5 cm in diameter. The computational domain and grid of the fluidization column correspond to the model representations (fig.2b) and have $\Delta r=0.75$ cm and $\Delta y=1$ cm.

To provide the gas velocity distribution along the radius of the column, the power law model was used in the following form [67]:

$$U_r = U_{max} [1 - (r/R)]^m \quad (25)$$

Fig. 4 shows the simplest case, when throughout the entire cross-section of the apparatus, the superficial gas velocity is constant, and diffusion migrations are prohibited in both the radial and radial directions ($D_{sr}=0$ m²/s, $D_{sa}=0$ m²/s). First, the fixed bed of particles occupies a certain number of cells in height (Fig. 3), while the concentration of particles is constant both in height and in width of the bed (with the exception of the upper cells of the bed, which are not completely filled). When the bed enters a fluidized state, the

particles occupy a larger number of cells, but the picture does not change qualitatively (Fig. 5).

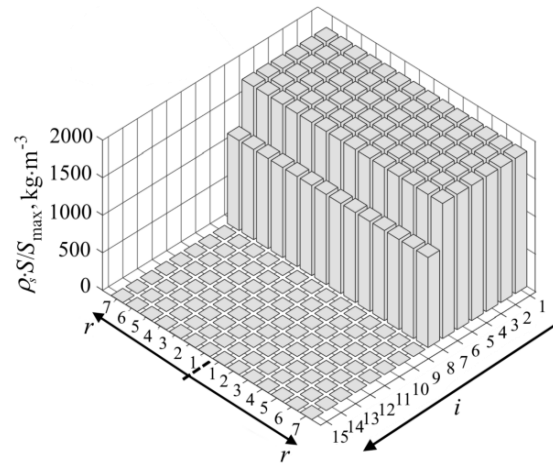


Fig. 4. The results of a numerical experiment with a uniform distribution of gas velocities over the cross section of the apparatus and in the absence of diffusion transfer ($D_{sa}=0$ m²/s; $D_{sr}=0$ m²/s) – distribution of volumetric density of particles for $k=1$ (fixed bed)

Qualitative changes occur when diffusion transfer is “turned on” (Fig. 6). Numerical values of the diffusion coefficients are not given here since they will be different for the different computational domains. The introduction of a non-zero axial diffusion coefficient makes the distribution of particle concentration along the height of the fluidized bed distinctly un-uniform, while a dense zone and a dilute zone can be distinguished (Fig. 6). Thus, it can be seen in Fig. 6 that the vertical distribution of particles has become quite plausible. In this case, each chain of cells is identical to the other (in other words, at the selected height, the same value of particle concentration is observed throughout the entire cross-section).

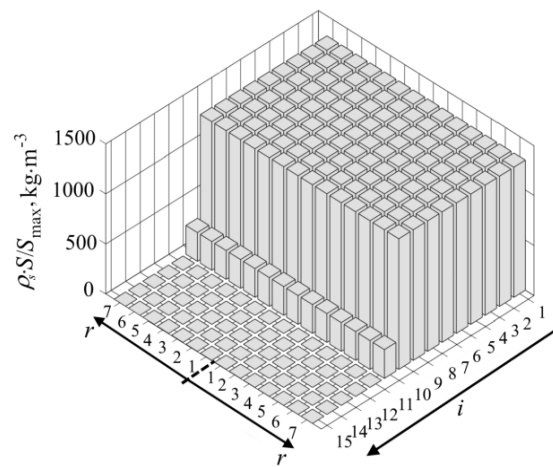


Fig. 5. The results of a numerical experiment with a uniform distribution of gas velocities over the cross section of the apparatus and in the absence of diffusion transfer ($D_{sa}=0$ m²/s; $D_{sr}=0$ m²/s) – distribution of volumetric density of particles for $k=2001$ (fluidized state at $t_k = (k - 1) \cdot \Delta t = 20$ s)

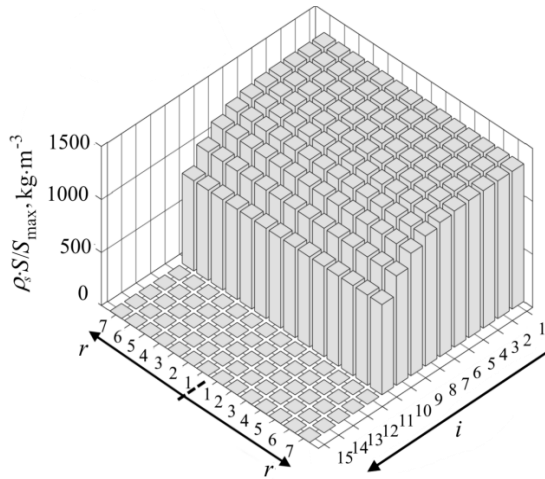


Fig. 6. Results of a numerical experiment with a uniform distribution of gas velocities over the cross section of the apparatus under different diffusion conditions (fluidized state at $t_k = (k - 1) \cdot \Delta t = 20$ s) – $D_{sa} > 0$ m²/s and $D_{sr} = 0$ m²/s

Since each chain of cells is identical to the neighboring chain of cells, the introduction of radial diffusion does not change the distribution (Fig. 7). Despite the fact that the distribution of particle concentrations in Fig. 7 remains unchanged (compared to Fig. 6), particle migrations into lateral direction occur, but their counter flows through any boundary between the computational domains compensate each other.

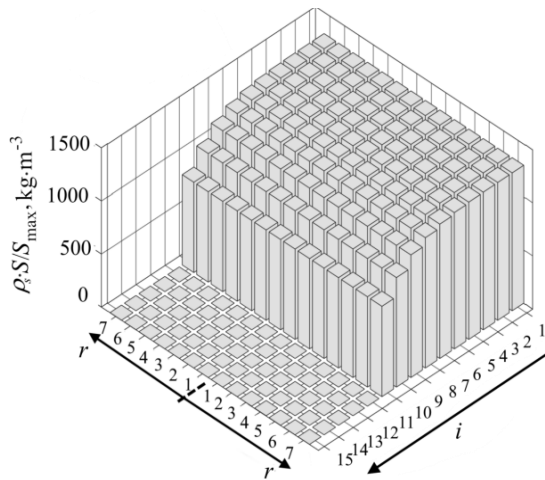


Fig. 7. Results of a numerical experiment with a uniform distribution of gas velocities over the cross section of the apparatus under different diffusion conditions (fluidized state at $t_k = (k - 1) \cdot \Delta t = 20$ s) – $D_{sa} > 0$ m²/s and $D_{sr} > 0$ m²/s

In order for the influence of diffusion flows in the radial direction to be obvious, it is necessary to initially work with a non-uniform radial profile of gas velocities. Figure 8a shows the distribution of particle concentrations obtained for the superficial gas velocity profile corresponding to $m=0.2$ in Eq. (5). The degree of non-uniformity of the velocity distribution for this case is shown in Fig. 8b.

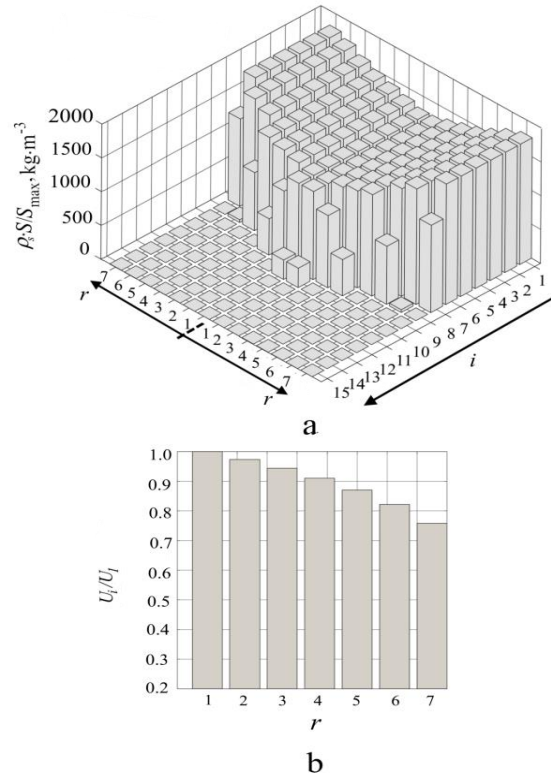


Fig. 8. Results of a numerical experiment with a non-uniform distribution of gas velocities over the cross section of the apparatus in the absence of diffusion transfer ($D_{sa} = 0$ m²/s and $D_{sr} = 0$ m²/s): a) solids distribution; b) degree of non-uniformity of the superficial gas velocity distribution

Results of fig. 9-10 show that diffusion as a process leads to some equalization of the particulate concentration. Thus the struggle between non-uniform distribution of the solid phase (created by the uneven profile of gas velocities) and diffusion processes in the radial and axial directions leads to the appearance of a completely qualitatively consistent distribution of the solid phase throughout the volume of the apparatus.

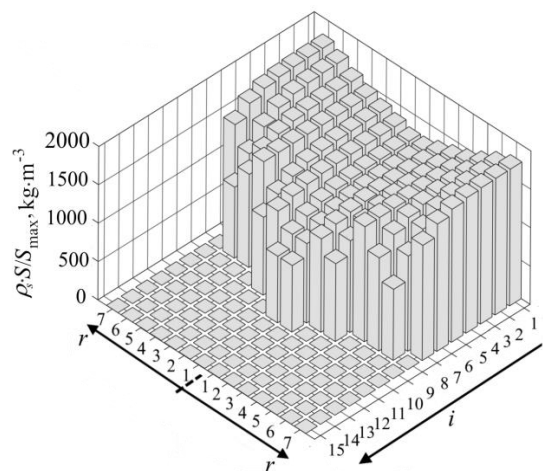


Fig. 9. Results of a numerical experiment with a non-uniform distribution of gas velocities over the cross section of the apparatus in the presence of diffusion transfer (fluidized state at $t_k = (k - 1) \cdot \Delta t = 20$ s): $D_{sa} > 0$ m²/s and $D_{sr} = 0$ m²/s

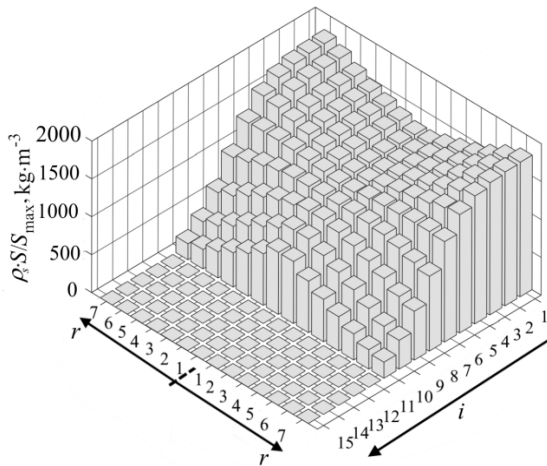


Fig. 10. Results of a numerical experiment with a non-uniform distribution of gas velocities over the cross section of the apparatus in the presence of diffusion transfer (fluidized state at $t_k = (k - 1) \cdot \Delta t = 20$ s): $D_{so} > 0$ m²/s and $D_{sr} > 0$ m²/s

Several authors studied the particulate movement of Geldart B powders and came to the conclusion that it has certain qualitative characteristics. The authors have shown that in fluidized beds with aspect ratio greater than unity, the suspended particles move downwards in the regions close to the wall and upwards in the central regions of the bed. There are two regions of particulate circulation that can be observed in beds with an aspect ratio greater than unity. The first forms are near the distributor plate, and the second forms are above the bed, near the top. At higher gas flow rates, the top region becomes more vigorous and dominates the entire solid mixing process [68, 69]. In figure 10, we can observe a similar situation obtained in a numerical experiment: in the central part of the bed, particles are more likely to move upward, while in the peripheral part of the bed, movement is more likely to be downward.

5.2. Experimental Results

Fig. 11-12 shows the results of the comparison of the results of the natural experiment (markers) and the calculated forecasts (lines). The parameters of the numerical model were brought into line with the physical parameters of the experiment described in the corresponding section of the article earlier. In this case, the computational grids $\Delta y = 0.05$ and $\Delta x = 0.005$ were used. The non-uniformity of the gas flow in the apparatus was characterized by the exponent $m = 1/7$ (eq. (25)) since this value corresponds to the physics of the process to a greater extent [67, 70]. However, it should be noted that m remains the calibration parameter of the model.

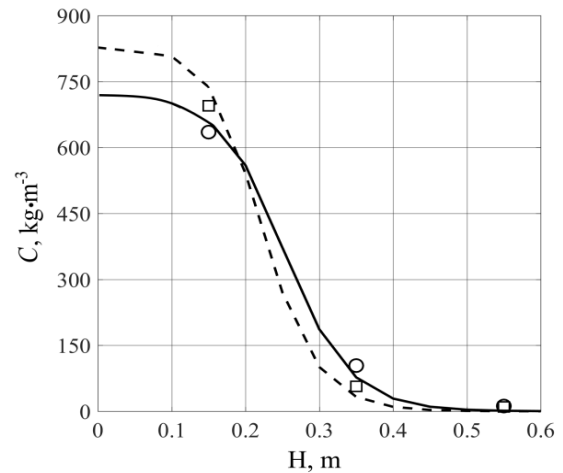


Fig. 11. Comparison of calculated (lines) and experimental (markers) particle concentration profiles after 10 min of fluidized bed drying: on the column axis (solid line, round marker) and at a distance of 2.5 cm from the column axis (dotted line, square marker)

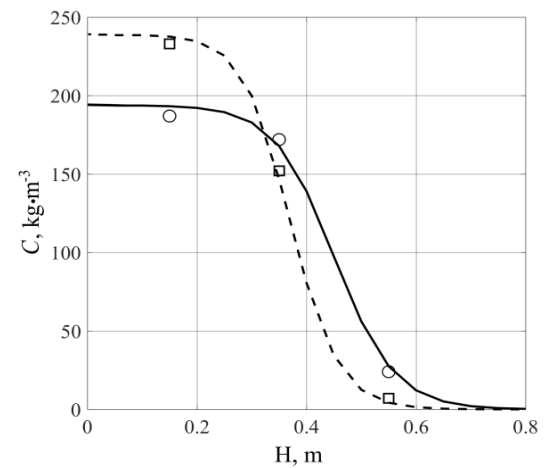


Fig. 12. Comparison of calculated (lines) and experimental (markers) particle concentration profiles after 55 min of fluidized bed drying: on the column axis (solid line, round marker) and at a distance of 2.5 cm from the column axis (dotted line, square marker)

From the fig. 11-12, it is evident that the model has sufficient predictive efficiency (the error at all points considered does not exceed 5-6%), while it should be noted that the parameter m (equation (25)) is actually the calibration parameter. In addition, it is noteworthy that the model underestimates the values in the lower part of the fluidized bed, which may be due to the influence of the gas distribution device. In any case, these findings should be considered preliminary, and further experimental studies are necessary.

6. Conclusions

In the present study, the cell mathematical model was first proposed to describe the motion of phases in a batch cylindrical column with a bubbling fluidized bed.

The main achieved results of the study, which have sufficient novelty, should be noted as follows:

1. the development of the two-dimensional mathematical cellular-type model of a batch fluidized bed column to describe the movement of bed components in radial and axial directions;
2. determination of the connection between the parameters of the proposed mathematical model and the physical parameters of the phase motion in the fluidized bed;
3. verification of the developed model by comparing the obtained simulations with the experimental data independent of the model.

As comments to the above points, the following circumstances should also be noted.

The phase transport of the fluidized bed along the height of the column are described on the basis of the mathematical apparatus of the theory of Markov chains, and an explicit difference scheme is used for the mathematical model of particle transfer in the radial direction.

This calculation scheme has apparently been applied for the first time, and the shape of the elementary representative volume is such that it corresponds to the established tradition of describing the mixing of particles during fluidization through radial and axial macrodiffusion components. The latter circumstance made it possible to greatly simplify the parametric identification procedure and perform it on the basis of calculation dependencies known from the literature.

The simplicity of the identification procedures, as well as the computational accessibility (not going beyond the capabilities of office computers), make the proposed model much more widely accessible for engineering practice than, for example, models based on DEM-CFD. At the same time, the model supports an intermediate scale of modeling. This scale of modeling allows us to consider the formation of the structure of a fluidized bed as an object with distributed spatial characteristics.

The main objectives of further work with the proposed mathematical model are:

- 1) changing the calculation scheme of the model in order to include the formation of gas bubbles in the calculation;
- 2) comprehensive testing of the model in various fluidization modes;
- 3) development of heat and mass transfer models in a fluidized bed based on the proposed fluidization model.

Nomenclature

| | |
|-----------|--|
| b | Probability of moving back to the located below cell |
| d | Diffusion transfer probability |
| d_1 | Particle diameter [m] |
| D_{sa} | Axial dispersion coefficient [m ² /s] |
| D_{sr} | Lateral dispersion coefficient [m ² /s] |
| f | Area of the largest cross-section of a particle perpendicular to the velocity vector [m ²] |
| F | Source vector of the gas flow [m ²] |
| Fr | Froude number |
| H | Height of the column [m] |
| k | Time step number |
| m | Parameter in Eq. (25) |
| N | Total number of the cylindrical layers |
| n | Total number of the cells in a Markovian chain |
| P | Transition matrix for solid |
| P_g | Transition matrix for gas |
| p | Probability for particle to staying in the same cell |
| Re | Reynolds number |
| r | Radial coordinate [m] |
| R | Column radius [m] |
| S_{max} | Maximum cell capacity [m ³] |
| S | State vector [m ³] |
| t | Time [s] |
| u | Probability for particle to moving upwards to the located above cell |
| V | Settling velocity of the particle [m/s] |
| U | Local gas velocity [m/s] |
| U_0 | Superficial gas velocity [m/s] |
| U_{mf} | Minimum fluidization velocity [m/s] |
| ρ | Density [kg/m ³] |

Subscripts

| | |
|-----|---------------------------------|
| g | Gas phase |
| i | Number of the cell number |
| k | Number of time step |
| r | Number of the cylindrical layer |
| s | Solid phase |

Funding Statement

This research did not receive any specific grant from funding agencies in the public, commercial, or not-for-profit sectors.

Conflicts of Interest

The author declares that there is no conflict of interest regarding the publication of this article.

Authors Contribution Statement

Andrey Mitrofanov: Conceptualization; Formal Analysis; Numerical Implementation; Experimental Validation; Writing and Design of the Manuscript.

References

- [1] De Munck, M.J.A., Peters, E.A.J.F., Kuipers, J.A.M. 2023. Fluidized bed gas-solid heat transfer using a CFD-DEM coarse-graining technique. *Chemical Engineering Science*, 280, 119048. doi: <https://doi.org/10.1016/j.ces.2023.119048>.
- [2] Deen, N.G., Van Sint Annaland, M., Van der Hoef, M.A., Kuipers, J.A.M. 2007. Review of discrete particle modeling of fluidized beds. *Chemical Engineering Science*, 62, pp. 28–44. doi: <https://doi.org/10.1016/j.ces.2006.08.014>.
- [3] Davidson, J.F., Harrison, D., 1971. *Fluidization*, Academic Press, London, New York.
- [4] Balag, J., Franco, D.A.T., Miral, V.G., Reyes, V., Tongco, L.J., Lopez, E.C.R., 2023. Recent Advances in Particle Fluidization. *ASEC 2023*, 62. doi: <https://doi.org/10.3390/ASEC2023-15321>.
- [5] Chen, C., 2016. Investigations on Mesoscale Structure in Gas-Solid Fluidization and Heterogeneous Drag Model, in: Springer Berlin Heidelberg, Berlin, Heidelberg, doi: <https://doi.org/10.1007/978-3-662-48373-2>.
- [6] Wang, J., Ren, C., Yang, Y., Hou, L., 2009. Characterization of Particle Fluidization Pattern in a Gas Solid Fluidized Bed Based on Acoustic Emission (AE) Measurement. *Ind. Eng. Chem. Res.*, 48, pp. 8508–8514. doi: <https://doi.org/10.1021/ie8018774>.
- [7] Van Der Hoef, M.A., Ye, M., Van Sint Annaland, M., Andrews, A.T., Sundaresan, S., Kuipers, J.A.M., 2006. Multiscale Modeling of Gas-Fluidized Beds. *Advances in Chemical Engineering*, 31, pp. 65–149. doi: [https://doi.org/10.1016/S0065-2377\(06\)31002-2](https://doi.org/10.1016/S0065-2377(06)31002-2).
- [8] Di Renzo, A., Scala, F., Heinrich, S., 2021. Recent Advances in Fluidized Bed Hydrodynamics and Transport Phenomena—Progress and Understanding. *Processes*, 9, (2021)639. doi: <https://doi.org/10.3390/pr9040639>.
- [9] Lettieri, P., Mazzei, L., 2009. Challenges and Issues on the CFD Modeling of Fluidized Beds: A Review. *The Journal of Computational Multiphase Flows*, 1, pp. 83–131. doi: <https://doi.org/10.1260/175748209789563937>.
- [10] Patterson, E.E., Halow, J., Daw, S., 2010. Innovative Method Using Magnetic Particle Tracking to Measure Solids Circulation in a Spouted Fluidized Bed. *Ind. Eng. Chem. Res.*, 49, pp. 5037–5043. doi: <https://doi.org/10.1021/ie9008698>.
- [11] Grace, J.R., 1997. *Circulating fluidized beds*, 1st ed., Blackie Academic & Professional, London, New York.
- [12] Esin, A., Altun, M., 1984. Correlation of axial mixing of solids in fluidized beds by a dispersion coefficient. *Powder Technology*, 39, pp. 241–244. doi: [https://doi.org/10.1016/0032-5910\(84\)85041-X](https://doi.org/10.1016/0032-5910(84)85041-X).
- [13] Geldart, D., 1973. Types of gas fluidization. *Powder Technology*, 7, (1973)pp. 285–292. doi: [https://doi.org/10.1016/0032-5910\(73\)80037-3](https://doi.org/10.1016/0032-5910(73)80037-3).
- [14] Shaul, S., Rabinovich, E., Kalman, H., 2014. Typical Fluidization Characteristics for Geldart's Classification Groups. *Particulate Science and Technology*, 32, pp. 197–205. doi: <https://doi.org/10.1080/02726351.2013.842624>.
- [15] Cocco, R., Chew, J.W., 2023. 50 years of Geldart classification. *Powder Technology*, 428, 118861. doi: <https://doi.org/10.1016/j.powtec.2023.118861>.
- [16] Drake, J.B., Heindel, T.J., 2012. Comparisons of Annular Hydrodynamic Structures in 3D Fluidized Beds Using X-Ray Computed Tomography Imaging. *Journal of Fluids Engineering*, 134, 081305. doi: <https://doi.org/10.1115/1.4007119>.
- [17] Sun, J., Yan, Y., 2016. Non-intrusive measurement and hydrodynamics characterization of gas–solid fluidized beds:

- a review. *Meas. Sci. Technol.*, 27, 112001. doi: <https://doi.org/10.1088/0957-0233/27/11/112001>.
- [18] Errigo, M., Windows-Yule, C., Materazzi, M., Werner, D., Lettieri, P., 2024. Non-invasive and non-intrusive diagnostic techniques for gas-solid fluidized beds – A review. *Powder Technology*, 431, 119098. doi: <https://doi.org/10.1016/j.powtec.2023.119098>.
- [19] Golshan, S., Sotudeh-Gharebagh, R., Zarghami, R., Mostoufi, N., Blais, B., Kuipers, J.A.M., 2020. Review and implementation of CFD-DEM applied to chemical process systems. *Chemical Engineering Science*, 221, 115646. doi: <https://doi.org/10.1016/j.ces.2020.115646>.
- [20] Mladenovic, M., Nemoda, S., Paprika, M., Marinkovic, A., 2019. Application of analytical and CFD models of liquid fuels combustion in a fluidized bed. *Therm Sci.*, 23, pp. 1627–1636. doi: <https://doi.org/10.2298/TSCI180226317M>.
- [21] Ma, H., Zhou, L., Liu, Z., M Chen, M., Xia, X., Zhao, Y., 2022. A review of recent development for the CFD-DEM investigations of non-spherical particles. *Powder Technology*, 412 117972. doi: <https://doi.org/10.1016/j.powtec.2022.117972>.
- [22] Berthiaux, H., Mizonov, V., Zhukov, V., 2005. Application of the theory of Markov chains to model different processes in particle technology. *Powder Technology*, 157, pp. 128–137. doi: <https://doi.org/10.1016/j.powtec.2005.05.019>.
- [23] Berthiaux, H., Mizonov, V., 2008. Applications of Markov Chains in Particulate Process Engineering: A Review. *Can. J. Chem. Eng.*, 82, pp. 1143–1168. doi: <https://doi.org/10.1002/cjce.5450820602>.
- [24] Dehling, H.G., Hoffmann, A.C., Stuu, H.W., 1999. Stochastic Models for Transport in a Fluidized Bed. *SIAM J. Appl. Math.*, 60, pp. 337–358. doi: <https://doi.org/10.1137/S0036139996306316>.
- [25] Cronin, K., Catak, M., Bour, J., Collins, A., Smee, J., 2011. Stochastic modelling of particle motion along a rotary drum. *Powder Technology*, 213, pp. 79–91. doi: <https://doi.org/10.1016/j.powtec.2011.07.009>.
- [26] Li, J., Huang, W., 2018. From Multiscale to Mesoscience: Addressing Mesoscales in Mesoregimes of Different Levels. *Annu. Rev. Chem. Biomol. Eng.*, 9, pp. 41–60. doi: <https://doi.org/10.1146/annurev-chembioeng-060817-084249>.
- [27] Di Renzo, A., Napolitano, E., Di Maio, F., 2021. Coarse-Grain DEM Modelling in Fluidized Bed Simulation: A Review. *Processes*, 9, 279. doi: <https://doi.org/10.3390/pr9020279>.
- [28] Catak, M., Cronin, K., Medina-Tellez, D., 2011. Markov Chain Modeling of Fluidized Bed Granulation Incorporating Simultaneous Aggregation and Breakage. *Ind. Eng. Chem. Res.*, 50, pp. 10811–10823. doi: <https://doi.org/10.1021/ie102513v>.
- [29] Li, J., Kwauk, M., 2001. Multiscale Nature of Complex Fluid-Particle Systems. *Ind. Eng. Chem. Res.*, 40, pp. 4227–4237. doi: <https://doi.org/10.1021/ie0011021>.
- [30] Lu, B., Niu, Y., Chen, F., Ahmad, N., Wang, W., Li, J., 2019. Energy-minimization multiscale based mesoscale modeling and applications in gas-fluidized catalytic reactors. *Reviews in Chemical Engineering*, 35, pp. 879–915. doi: <https://doi.org/10.1515/revce-2017-0023>.
- [31] Zhuang, Y., Chen, X., Liu, D., 2016. Stochastic bubble developing model combined with Markov process of particles for bubbling fluidized beds. *Chemical Engineering Journal*, 291, pp. 206–214. doi: <https://doi.org/10.1016/j.ces.2016.01.095>.
- [32] Hernández-Jiménez, F., Sánchez-Delgado, S., Gómez-García, A., Acosta-Iborra, A., 2011. Comparison between two-fluid model simulations and particle image analysis & velocimetry (PIV) results for a two-dimensional gas-solid fluidized bed. *Chemical Engineering Science*, 66, pp. 3753–3772. doi: <https://doi.org/10.1016/j.ces.2011.04.026>.
- [33] Link, J., Zeilstra, C., Deen, N., Kuipers, H., 2008. Validation of a Discrete Particle Model in a 2D Spout-Fluid Bed Using Non-Intrusive Optical Measuring Techniques. *Can. J. Chem. Eng.*, 82, pp. 30–36. doi: <https://doi.org/10.1002/cjce.5450820105>.
- [34] Ismail, T.M., Abd El-Salam, M., Monteiro, E., Rouboa, A., 2016. Eulerian – Eulerian CFD model on fluidized bed gasifier using coffee husks as fuel. *Applied Thermal Engineering*, 106, pp. 1391–1402. doi: <https://doi.org/10.1016/j.applthermaleng.2016.06.102>.
- [35] Reddy, P.N., Verma, V., Kumar, A., Awasthi, M.K., 2023. CFD Simulation and Thermal

- Performance Optimization of Channel Flow with Multiple Baffles. *Journal of Heat and Mass Transfer Research*, 10, pp. 257–268. doi: <https://doi.org/10.22075/jhmtr.2023.31108.1458>.
- [36] Vahedi, S.M., Parvaz, F., Rafee, R., Khandan Bakavoli, M., 2018. Computational fluid dynamics simulation of the flow patterns and performance of conventional and dual-cone gas-particle cyclones. *Journal of Heat and Mass Transfer Research*, 5, pp. 27–38. doi: <https://doi.org/10.22075/jhmtr.2017.11918.1170>.
- [37] Zhonghua, W., Mujumdar, A.S., 2008. CFD modeling of the gas–particle flow behavior in spouted beds. *Powder Technology*, 183, 260–272. doi: <https://doi.org/10.1016/j.powtec.2007.07.040>.
- [38] Feng, Y.Q., Xu, B.H., Zhang, S.J., Yu, A.B., Zulli, P., 2004. Discrete particle simulation of gas fluidization of particle mixtures. *AIChE Journal*, 50, pp. 1713–1728. doi: <https://doi.org/10.1002/aic.10169>.
- [39] Zhao, Y., Shi, X., Wang, C., Lan, X., Gao, J., 2023. Study on flow characteristics of turbulent fluidized bed with variable gas velocity due to chemical reactions. *Powder Technology*, 416, 118211. doi: <https://doi.org/10.1016/j.powtec.2022.118211>.
- [40] Liu, F., Li, C., Zeng, X., Chen, J., Guan, J., Yang, L., 2024. Study on the flow and collision characteristics of catalyst particles in FCC reactor. *Powder Technology*, 438, 119642. doi: <https://doi.org/10.1016/j.powtec.2024.119642>.
- [41] Zhao, Y., Shi, X., Lan, X., Gao, J., Jing, W., Xiong, Q., 2024. Simulation analysis of micro-explosion during emulsification feeding of residue fluidized catalytic cracking. *Applied Thermal Engineering*, 250, 123514. doi: <https://doi.org/10.1016/j.applthermaleng.2024.123514>.
- [42] Ma, H., Zhao, Y., 2018. CFD-DEM investigation of the fluidization of binary mixtures containing rod-like particles and spherical particles in a fluidized bed. *Powder Technology*, 336, 533–545. doi: <https://doi.org/10.1016/j.powtec.2018.06.034>.
- [43] He, L., Liu, Z., Zhao, Y., 2022. An extended unresolved CFD-DEM coupling method for simulation of fluid and non-spherical particles. *Particuology*, 68, 1–12. doi: <https://doi.org/10.1016/j.partic.2021.11.001>.
- [44] Xu, J., Zhao, P., Zhang, Y., Wang, J., Ge, W., 2022. Discrete particle methods for engineering simulation: Reproducing mesoscale structures in multiphase systems. *Resources Chemicals and Materials*, 1, pp. 69–79. doi: <https://doi.org/10.1016/j.recem.2022.01.002>.
- [45] Liu, X., Zhu, A., Yang, L., Xu, J., Li, H., Ge, W., Ye, M., 2022. Numerical simulation of commercial MTO fluidized bed reactor with a coarse-grained discrete particle method — EMMS-DPM. *Powder Technology*, 406, 117576. doi: <https://doi.org/10.1016/j.powtec.2022.117576>.
- [46] Wang, T., Zhang, F., Furtney, J., Damjanac, B., 2022. A review of methods, applications and limitations for incorporating fluid flow in the discrete element method. *Journal of Rock Mechanics and Geotechnical Engineering*, 14, pp. 1005–1024. doi: <https://doi.org/10.1016/j.jrmge.2021.10.015>.
- [47] Gutsche, R., Hartmann, K., 1995. Application of Markov chains in deriving for predicting the dynamic behaviour of chemical engineering processes. *Computers & Chemical Engineering*, 19 pp. 729–734. doi: [https://doi.org/10.1016/0098-1354\(95\)87121-7](https://doi.org/10.1016/0098-1354(95)87121-7).
- [48] Tamir, A., 1998. Applications of Markov chains in chemical processes, in: Elsevier, pp. 498–589. doi: <https://doi.org/10.1016/B978-044482356-4/50007-9>.
- [49] Mitrofanov, A., Mizonov, V., Tannous, K., Ovchinnikov, L., 2018. A Markov chain model to describe fluidization of particles with time-varying properties. *Particulate Science and Technology*, 36, 244–253. doi: <https://doi.org/10.1080/02726351.2016.1243180>.
- [50] Sánchez-Prieto, J., Hernández-Jiménez, F., García-Gutiérrez, L.M., Soria-Verdugo, A., 2017. Experimental study on the characteristic mixing time of solids and its link with the lateral dispersion coefficient in bubbling fluidized beds. *Chemical Engineering Journal*, 307, pp. 113–121. doi: <https://doi.org/10.1016/j.cej.2016.08.075>.

- [51] Liu, D., Chen, X., 2010. Lateral solids dispersion coefficient in large-scale fluidized beds. *Combustion and Flame*, 157, pp. 2116–2124. doi: <https://doi.org/10.1016/j.combustflame.2010.04.020>.
- [52] Castilla, G.M., Larsson, A., Lundberg, L., Johnsson, F., Pallarès, D., 2020. A novel experimental method for determining lateral mixing of solids in fluidized beds – Quantification of the splash-zone contribution. *Powder Technology*, 370, pp. 96–103. doi: <https://doi.org/10.1016/j.powtec.2020.05.036>.
- [53] Bokkers, G.A., Van Sint Annaland, M., Kuipers, J.A.M., 2004. Mixing and segregation in a bidisperse gas–solid fluidised bed: a numerical and experimental study. *Powder Technology*, 140, pp. 176–186. doi: <https://doi.org/10.1016/j.powtec.2004.01.018>.
- [54] Sánchez-Prieto, J., Hernández-Jiménez, F., García-Gutiérrez, L.M., Soria-Verdugo, A., 2017. Experimental study on the characteristic mixing time of solids and its link with the lateral dispersion coefficient in bubbling fluidized beds. *Chemical Engineering Journal*, 307, pp. 113–121. doi: <https://doi.org/10.1016/j.cej.2016.08.075>.
- [55] Köhler, A., Rasch, A., Pallarès, D., Johnsson, F., 2017. Experimental characterization of axial fuel mixing in fluidized beds by magnetic particle tracking. *Powder Technology*, 316, pp. 492–499. doi: <https://doi.org/10.1016/j.powtec.2016.12.093>.
- [56] Rhodes, M.J., Wang, X.S., Nguyen, M., Stewart, P., Liffman, K., 2001. Study of mixing in gas-fluidized beds using a DEM model. *Chemical Engineering Science*, 56, pp. 2859–2866. doi: [https://doi.org/10.1016/S0009-2509\(00\)00524-8](https://doi.org/10.1016/S0009-2509(00)00524-8).
- [57] Niklasson, F., Thunman, H., Johnsson, F., Leckner, B., 2002. Estimation of Solids Mixing in a Fluidized-Bed Combustor. *Ind. Eng. Chem. Res.*, 41, pp. 4663–4673. doi: <https://doi.org/10.1021/ie020173s>.
- [58] Borodulya, V.A., Epanov, Yu.G., Teplitskii, Yu.S., 1982. Horizontal particle mixing in a free fluidized bed. *Journal of Engineering Physics*, 42, pp. 528–533. doi: <https://doi.org/10.1007/BF00824945>.
- [59] Mizonov, V., Mitrofanov, A., Ogurtsov, A., Tannous, K., 2014. Modeling of Particle Concentration Distribution in a Fluidized Bed by Means of the Theory of Markov Chains. *Particulate Science and Technology*, 32, pp. 171–178. doi: <https://doi.org/10.1080/02726351.2013.839016>.
- [60] Mitrofanov, A.V., Mizonov, V.E., Shpeynova, N.S., Vasilevich, S.V., Kasatkina, N.K., 2021. Experimental and Theoretical Study of the Axial Distribution of Solid Phase Particles in a Fluidized Bed, *Energetika. Proceedings of CIS Higher Education Institutions and Power Engineering Associations*, 64, pp. 349–362. doi: <https://doi.org/10.21122/1029-7448-2021-64-4-349-362>.
- [61] Mitrofanov, A., Vasilevich, S., Mal'ko, M., Ogurtsov, A., Shpeynova, N., 2023. Design and verification of the model of structure formation and heat transfer in a fluidized bed apparatus with a heat jacket. *ChemChemTech.*, 5, pp. 128–138. doi: <https://doi.org/10.6060/ivkkt.20236605.6748>.
- [62] Li, R., Huang, X., Wu, Y., Dong, L., Belošević, S., Milićević, A., Tomanović, I., Deng, L., Che, D., 2023. Comparative analysis on gas–solid drag models in MFIX-DEM simulations of bubbling fluidized bed. *Chinese Journal of Chemical Engineering*, 64, pp. 64–75. doi: <https://doi.org/10.1016/j.cjche.2023.06.002>.
- [63] Mikhailov, M.D., Freire, A.P.S., The drag coefficient of a sphere: An approximation using Shanks transform. 2013. *Powder Technology*, 237, pp. 432–435. doi: <https://doi.org/10.1016/j.powtec.2012.12.033>.
- [64] Khan, A.R., Richardson, J.F., 1987. The resistance to motion of a solid sphere in a fluid. *Chemical Engineering Communications*, 62, pp. 135–150. doi: <https://doi.org/10.1080/00986448708912056>.
- [65] Mitrofanov, A., Ovchinnikov, L., Ovchinnikov, N., Ogurtsov, A., Lapshina, O., 2022. Computational and experimental study of the thermal process in an individual cylindrical particle. *ChemChemTech.*, 65, pp. 97–104. doi: <https://doi.org/10.6060/ivkkt.20226509.6679>.
- [66] Muir, C.E., Lowry, B.J., Balcom, B.J., 2011. Measuring diffusion using the differential form of Fick's law and magnetic resonance

- imaging. *New J. Phys.*, 13, 015005. doi: <https://doi.org/10.1088/1367-2630/13/1/015005>.
- [67] Chanson, H., 2009. *Applied Hydrodynamics: An Introduction to Ideal and Real Fluid Flows*, in: 0 ed., CRC Press, p. 464. doi: <https://doi.org/10.1201/b11464>.
- [68] Lin, J.S., Chen, M.M., Chao, B.T., 1985. A novel radioactive particle tracking facility for measurement of solids motion in gas-fluidized beds. *AIChE Journal*, 31, pp. 465–473. doi: <https://doi.org/10.1002/aic.690310314>.
- [69] Yamazaki, R., Ueda, N., Jimbo, G., 1986. Mechanism of incipient fluidization in fluidized bed at elevated temperature. *Journal of Chemical Engineering of Japan*, 19, pp. 251–257.
- [70] De Chant, L.J., 2005. The venerable 1/7th power law turbulent velocity profile: a classical nonlinear boundary value problem solution and its relationship to stochastic processes. *Applied Mathematics and Computation*, 161, pp. 463–474. doi: <https://doi.org/10.1016/j.amc.2003.12.109>.